

Water structure changes induced by hydrophobic and polar solutes revealed by simulations and infrared spectroscopy

Kim A. Sharp,^{a)} Bhupinder Madan, Eric Manas, and Jane M. Vanderkooi
E. R. Johnson Research Foundation, Department of Biochemistry and Biophysics, University of Pennsylvania, 37th and Hamilton Walk, Philadelphia, Pennsylvania 10104-6059

(Received 25 May 2000; accepted 31 October 2000)

A combination of simulations and Fourier transform infrared spectroscopy was used to examine the effect of three ionic solutes (KCl, NaCl, and KSCN), the polar solute urea, and the osmolyte trimethylamine-N-oxide (TMAO) on a water structure. The ionic solutes increase the mean water–water H-bond angle in their first hydration shell concomitantly shifting the OH stretching mode to higher frequency, and shifting the HOH bending mode to lower frequency. TMAO decreases the mean water–water H-bond angle in its first hydration shell, shifts the OH stretching mode frequency down, and shifting the HOH bending mode frequency up. Urea has no effect on the mean H-bond angle, OH stretch, and HOH bend frequencies. These results can be explained in terms of changes in the relative proportions of two H-bond angle populations: Ionic solutes increase the population of more distorted (larger angle) H bonds relative to the less distorted population, TMAO has the reverse effect, while urea does not affect the H-bond angle probability distribution. The negligible effect of urea on water structure supports the direct binding model for urea-induced protein denaturation. © 2001 American Institute of Physics. [DOI: 10.1063/1.1334678]

I. INTRODUCTION

Water is a highly structured liquid with many interesting physical properties that have yet to be explained at a molecular level. Ionic, polar, and hydrophobic solutes perturb the structure of water in different ways with profound consequences for their solubility, hydration thermodynamics, and their association with other solutes. Solute-induced perturbations in water structure are, in turn, less well understood than the structure of pure water. One of the most important features of liquid water is the high degree of orientational, or angular, ordering that results in an open, low coordination number structure.¹ In a series of simulation studies of solute hydration we have shown that solute-induced perturbations of a water structure are manifest primarily in the distribution of the angles of hydrogen bonds (H bonds) between waters within the first hydration shell.^{2–6}

These simulations reveal that in bulk water (coordination number ≈ 4.8 at 20 °C) the H-bond angle distribution is bimodal with, on average, about four nearly linear ($\theta_h \approx 12^\circ$) H bonds and 0.8 more bent ($\theta_h \approx 52^\circ$) H bonds. (In these studies the H-bond angle θ_h is defined by the smallest O··O–H angle formed by two neighboring waters, with a linear H bond having an angle of 0°.) Hydrophobic solutes and solute groups decrease the root mean square (rms) H-bond angle, θ , between waters in their first hydration shell. This familiar increase in “icelike” water structuring is not, however, achieved by straightening the H bonds but by decreasing the population of more distorted (higher angle) H bonds relative to the less distorted population. This is primarily a geometric effect since nonpolar solutes can interact only weakly and nondirectionally with water through van der

Waals interactions. A more bent H bond indicates a more weakly interacting water, which is more easily displaced by a nonpolar solute.⁵

Polar and ionic solute groups have the opposite effect, increasing the rms H-bond angle by increasing the population of more distorted H bonds at the expense of the less distorted population. This is primarily an electrostatic effect on the water dipole orientation. These angular changes cause concomitant decreases and increases in the rms H-bond length between first shell waters around hydrophobic and polar solutes, respectively, but these are much smaller than the angular perturbations. Since H-bond angle and length are highly correlated one can effectively describe both hydrophobic and polar solute-induced distortion of water by a single “structural distortion coordinate,” namely the rms angle of the H bond between waters in the first shell.

These changes in water orientational structure caused by shifts between populations of “less distorted” or “more distorted” H bonds can quantitatively explain hydration heat capacity (ΔC_p) changes for a variety of polar, ionic, and hydrophobic solutes.⁵ In previous work we focused on explaining ΔC_p in structural and molecular terms since, unlike hydration entropies and hydration enthalpies, ΔC_p differs in sign between polar and hydrophobic solutes and thus it more closely reflects the qualitative difference in the solvation structure between polar and apolar groups.

Neutron scattering experiments show a surprisingly small degree of water structure ordering around tetra-alkyl ammonium ions (ions that show “apolarlike” hydration and that can form crystalline clathrate hydrates).^{7–9} Our simulations also provide an explanation for this. These scattering experiments provide information about radial distribution functions between water atoms. Simulations show that the

^{a)}Electronic mail: SHARPK@MAIL.MED.UPENN.EDU

radial distribution functions are relatively insensitive to the effects of the solute, whereas significant angular structure perturbations can lie under very similar radial distribution function envelopes.⁴ The conclusion is that solute-induced distortions of a water structure are manifest primarily in the distribution of hydrogen bond angles between first shell waters with little change in H-bond distances.

Although we can provide satisfactory explanations of the thermodynamic and neutron scattering data, it would be desirable to obtain more direct experimental measures of such angular structure perturbations in water. Fourier transform infrared spectroscopy (FTIR) of water in the presence and absence of solutes can, in principle, provide such information. Consider first the O–H stretch of water: It is well known that if the H atom forms a hydrogen bond to a second water the vibrational frequency decreases relative to that in the gas phase. This can be explained qualitatively as a consequence of the second oxygen flattening the effective potential well in which the H atom sits with respect to displacements along the O–H bond. Conversely, for the H–O–H bend, H-bond formation increases the frequency, since the second oxygen provides an additional restoring force with respect to displacements of the H atom normal to the O–H bond. If we now consider the effect of distorting the H bond by bending (and lengthening) it, this attenuates the effect of the second oxygen, i.e., it will diminish the downward shift for the O–H stretch, and diminish the upward shift for the H–O–H bend. Thus, the expectation is that if distortions in the water structure caused by hydrophobic solutes or solute groups decrease the mean water–water H-bond angle, this, in turn, will result in a shift to lower frequency in the O–H stretch and an upward shift in the H–O–H bend, respectively, which could be detected by FTIR spectroscopy. Conversely, if polar solutes or solute groups increase the mean water–water H-bond angle, this would cause a shift to higher frequency in the O–H stretch and a downward shift in the H–O–H bend, respectively. To test this hypothesis we carried out a combination of simulations and FTIR spectroscopic measurements.

In this paper, we examine the effect of three ionic solutes (KCl, NaCl, and KSCN), the polar solute urea, and the osmolyte trimethylamine-N-oxide. A major difficulty in studying the effect of apolar solutes on water has, of course, been their low solubility. In this case any experimental signal—IR or otherwise—from the perturbed hydrating waters is masked by the much larger contribution from bulk water. Previous studies have addressed this solubility problem using the hydrophobic (i.e., having a positive ΔC_p of hydration) tetra-alkyl ammonium ions.⁷ These ions are highly soluble in water, but a nonhydrophobic counterion is always present. In this study we chose to use TMAO, which is nonionic, highly soluble, but contains three hydrophobic methyl groups and, judged by its positive hydration heat capacity¹⁰ has a net “hydrophobelike” effect on the water structure. Urea and TMAO are also of particular interest in the context of water structure because of their effect upon protein stability: Urea has a large destabilizing effect, while TMAO is the most effective known osmolyte at stabilizing proteins.¹¹ It has been proposed that urea can weaken the

hydrophobic effect by decreasing the water structure, thus destabilizing proteins. If such a mechanism is in operation, the possibility exists that stabilizing osmolytes like TMAO can act by opposing effects on water structure. These kinds of hypotheses about water structure have not yet been verified, but are examined here using a combination of simulation and FTIR spectroscopy.

II. METHODS

A. Materials

Water was deionized and then glass distilled, D₂O and all other chemicals were obtained from the Sigma-Aldrich Chemical Company (St. Louis, MO). The protons of urea were exchanged for deuterons by dissolving the solid urea into D₂O, and then evaporating the solvent. To avoid proton exchange from atmospheric water vapor, the solid residue was immediately used to make the urea solution.

B. Spectroscopic methods

Infrared (IR) spectra were obtained with a Bruker IFS 66 FTIR spectrometer (Bruker Inc., Brookline, MA), configured with a Globar source and a KBr beamsplitter, and a liquid nitrogen cooled HgCdTe (MCT) detector.¹² The spectral resolution was 0.5 cm⁻¹. Following data acquisition and subtraction of the background the data were convolved to give 2 cm⁻¹ resolution. The spectra were taken in the transmission mode, and the spacer was 6 μ . Deconvolution of the spectra was performed using the PeakFit software package (Jandel Scientific Software, CA).

C. Theoretical methods

Aqueous solutions of each of the following solutes: trimethylamine oxide (TMAO), and ions of the three salts, potassium thiocyanate (KSCN), sodium chloride (NaCl), and potassium chloride (KCl) were simulated by inserting one molecule/ion of each of these solutes into a box of 750 TIP4P waters. The box dimensions were 37.5 Å × 25 Å × 25 Å. Periodic boundary conditions were used with a cutoff of 12.0 Å. The urea solution was simulated using a 25 Å × 25 Å × 25 Å box containing 216 TIP4P waters. The OPLS parameters were used for the solutes.¹³ A Metropolis Monte Carlo algorithm incorporated in the program BOSS¹⁴ was used to run simulations at 25 °C and 1 atm. Further details of the simulations have been provided in our previous work.² An instantaneous snapshot of the system was analyzed every 1000 steps during each of the 10 data collection runs. Each run consisted of 1 × 10⁷ Monte Carlo steps. The error estimates for average quantities were computed over the ten runs.

For each solute atom the solute atom–water oxygen radial distribution function, $g(r)$, was computed, and then the first minimum in the solute atom–water oxygen radial distribution function was used to identify all first hydration shell waters. The first minimum in the pure water radial distribution function of pure water, which defines the first coordination shell of water, lies at 3.4 Å. Two first hydration shell water molecules closer than an oxygen–oxygen distance of

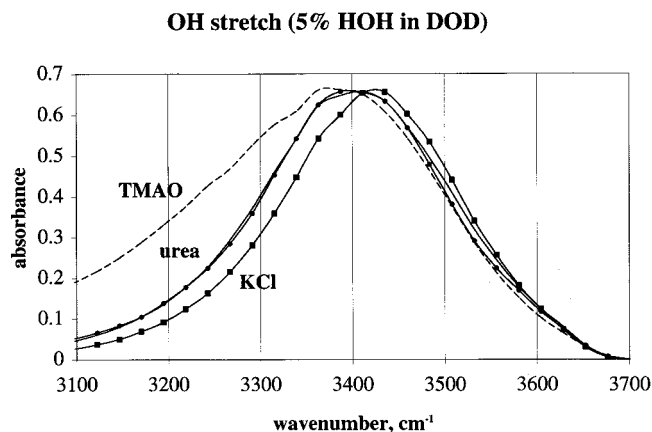


FIG. 1. OH stretching band for HOD at 25 °C. Pure solvent (5% H₂O and 95% D₂O): Solid line with no symbols. Solutions of KCl (■), TMAO (dashed line) or urea (●) in 5% H₂O and 95% D₂O as indicated in the figure.

3.4 Å are defined to be hydrogen bonded. The hydrogen bond angles and the oxygen–oxygen distances were binned into their respective probability distribution functions and used to compute the average random network model parameters: the mean hydrogen bond distance, d , and the root mean square hydrogen bond angle, θ . The hydrogen bonds formed between water molecules in the first hydration shells of the solute atoms can also be subdivided into various classes as follows. Each first shell water is assigned to its nearest solute atom. An intrasolute–atom class of hydrogen bonds would involve hydrogen bonds formed between two water molecules on same solute atom. An intersolute–atom class of hydrogen bond is formed between two water molecules on two different solute atoms or groups. For example, water–water hydrogen bonds around the TMAO molecule could be classified as CH₃–CH₃, CH₃–N, or CH₃–O, and so on, where CH₃–CH₃ refers to the hydrogen bonds formed between two water molecules, each solvating a methyl group. The class CH₃–N indicates hydrogen bonds formed between a water molecule on a CH₃ group and the second water molecule on the nitrogen atom of the solute, and so on. Hydrogen bonds belonging to each of such classes were counted for each configuration and were averaged over the whole run. In addition, d and θ were computed over the entire set of first shell water–water H bonds.

III. RESULTS

A. Infrared spectra

The OH stretching band of HOD in D₂O at 25 °C is shown in Fig. 1; this band is centered at 3407 cm⁻¹. With the addition of various strong electrolytes, including KCl, KSCN, and NaCl, this band shifts to higher frequency. The spectrum for the KCl solution is also shown in Fig. 1. A concentrated aqueous solution of TMAO was used to examine the effects of hydrophobic hydration on the water spectrum. As seen in Fig. 1, in contrast to the effects of strong electrolytes, the addition of TMAO causes the OH stretching band of water to shift to lower frequency. Very little shift was observed for the OH stretching band in the presence of

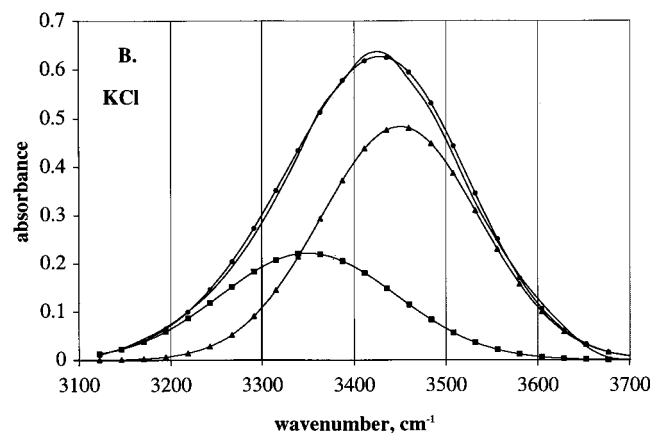
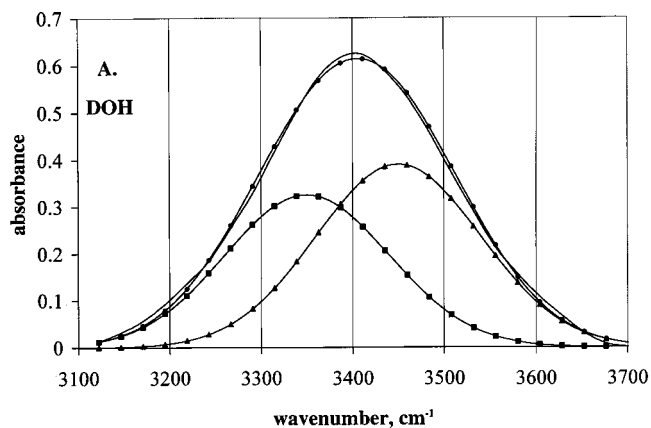


FIG. 2. An example of fits to two Gaussians. Squares represent a Gaussian centered at 3350 cm⁻¹ (width 210 cm⁻¹) and triangles are Gaussian centered at 3450 cm⁻¹ (width 212 cm⁻¹). Circles are the sum of the two Gaussians and the solid line is the observed experimental curve (from Fig. 1). (A) 5% H₂O and 95% D₂O. Respective areas of the fit components: 45% and 55%; (B) 4 molal KCl. Respective areas: 33% and 67%.

urea, within our experimental resolution, as is shown in Fig. 1. The only small, but reproducible effect is a slight narrowing of the band in the presence of urea. For a 5 M urea solution the concentration of NH in the solution will be approximately one-tenth that of OH. Since NH will be also contributing in this region, it may be contributing absorbance in the center of the peak. However, the same absorbance at the higher- and lower-energy sides of the absorbance band is evidence that urea is not significantly perturbing the water OH bonding.

As discussed in the Introduction, it is likely that the higher-frequency components of the OH stretching band represent more distorted hydrogen bonded species. Since polar and charged species act to distort H bonds, the addition of strong electrolytes to water would be expected to enhance the band(s) representing more weakly hydrogen bonded species, while the addition of hydrophobic groups would weaken the band(s), which is what we see experimentally. To put this interpretation on a more quantitative basis, we performed deconvolution of the spectra as follows. The pure water OH stretch frequency peak was fit with two Gaussians. (This peak cannot be fit satisfactorily by a single Gaussian function.) This produced an excellent fit ($R^2=0.999$, Fig. 2) for two Gaussians centered at 3350 and 3450 cm⁻¹, respec-

TABLE I. Effect of various solutes on an angle of O··O–H and IR OH stretch, ν_s , and bending (δb) frequencies for DOD and DOH in 95% D₂O/H₂O and various solutes.

Solute	N_{hb}	d (Å)	θ (°) ^a	Molality	Moles solvent/solute ^b	Ratio of 3350/3450 cm ⁻¹ peaks	δDOD cm ⁻¹	δDOH cm ⁻¹
None		2.94	29			45/54	1210	1461
KCl	6.2	3.13	55	4.4	6/1	33/66	1207	1450
NaCl	7.7	3.16	61	4.4	6/1	31/68	1208	1450
KSCN	27	3.00	37	4	7/1	36/63	1206	1449
TMAO	50	2.92	27	8	7/1	66/33	1238	1482
Urea	32	2.93	29	8	7/1	43/57	1210	N.D.

^a N_{hb} , d , and θ are the simulated mean number of H bonds, the mean length, and the rms angle, respectively, over all H bonds between first shell waters.

^bMoles water/moles molecule or ion.

tively. The OH stretch peak for all the solutions was then fit with two Gaussians centered at the *same* frequencies by varying their relative intensities. In all cases the fits had $R^2 \geq 0.997$. The single exception is TMAO solutions, which are fit well by two Gaussians, except for a low-frequency tail. It should be pointed out that these are not unique fits. Laenen *et al.*^{15,16} derived three major components in time-resolved spectra obtained from hole burning. Our data could also, for instance, be fit to the parameters that they used (i.e., 3350, 3400, and 3450 cm⁻¹). However, without further information, the fitting of our data to multiple functions is arbitrary. Further, fitting all the spectra to a pair of fixed frequency peaks allows one to analyze the frequency shifts observed in the spectra in a quantitative manner with a parsimonious introduction of adjustable parameters.

Using this analysis, for KCl solutions the component of the peak attributable to strongly hydrogen bonded species (the low-energy component centered at 3350 cm⁻¹) decreases in intensity with respect to the component attributable to weakly hydrogen bonded species (the higher-energy component centered at 3450 cm⁻¹). Similar effects were seen for NaCl and KSCN solutions. The component ratios are given in Table I. Since we expect TMAO to structure water in a more icelike way, and reduce the H-bond angle, it is consistent that the addition of TMAO to water leads to an enhancement of the lower-frequency band(s) representing more strongly hydrogen bonded species. This is borne out in the component ratio for the TMAO solution in Table I. There was, in addition, in the TMAO spectrum a broad lower-frequency component, as mentioned above; the fit centered it at 3200 cm⁻¹. Interestingly, a third component is also seen in ultrafast infrared hole burning experiments, and this component is believed to be icelike, but with large local fluctuations.¹⁶ Finally, the component ratio is unchanged by the addition of urea to water.

The effect of the solutes upon the bending modes of water was also monitored. The DOH and DOD bending modes were observed to shift to lower frequency upon the addition of any of the strong electrolytes (Table I). The relative effect of a solute is larger on the DOH bending frequency than the DOD bending frequency, but for all polar solutes a downward shift is observed. For urea, the DOH bending mode was not recorded because it was obscured by fingerprint modes of the urea, but the DOD bending mode is

unchanged from the 5% H₂O–95% D₂O solvent. TMAO causes an upward shift in the DOD and DOH bending frequencies.

The sample used for the above experiments was 95/5% DOD/HOD. At this ratio the HOH concentration is ~ 0.14 M and the HOD is ~ 5.3 M. Consequently, the major contributor to the spectral region examined is HOD, and because the vibrations are decoupled, the spectrum represents a simple OH stretch. The experiments were repeated at twice the amount of H₂O in the D₂O. The same results were obtained, showing that indeed we are observing the decoupled OH stretch band, without a significant contribution from coupled HOH stretching modes. We also examined the effect of these solutes on neat D₂O and H₂O. The results show the same trend as for the decoupled OH/OD stretch. For the TMAO solution, the components of the OD stretching band attributable to strongly hydrogen bonded species (the low-frequency components) increase in intensity with respect to the components attributable to weakly hydrogen bonded species (the higher-energy components). The OH/OD stretching band of the KCl solution showed the opposite trend. However, the stretching band region for neat solvents is a composite of symmetric and antisymmetric stretching modes overlaid on the effects of the more strongly and less strongly hydrogen bonded species. Thus deconvolution of these spectra is significantly more difficult, and we restrict our detailed analysis to the decoupled stretch case.

B. Simulations

From the simulations the mean number of water–water H bonds, and their mean length and rms angle were computed for pure water, and the first hydration shells of the solutes. The results are collected in Table I. Pure water has a rms H-bond angle of 29°. The probability distribution of the H-bond angles themselves is bimodal with peaks at $\approx 12^\circ$ and $\approx 52^\circ$ (Fig. 3). The addition of KCl, KSCN, or NaCl results in a large increase in the rms angle. This increase results from a shift in population from the low angle peak to the high angle peak. This is illustrated in Fig. 3 for the KCl solution. Here the low angle peak is nearly eliminated, indicating a large angular distortion in the first shell water structure. Results for the other salts (not shown) are very similar. For the TMAO solution, the rms angle decreases. This is

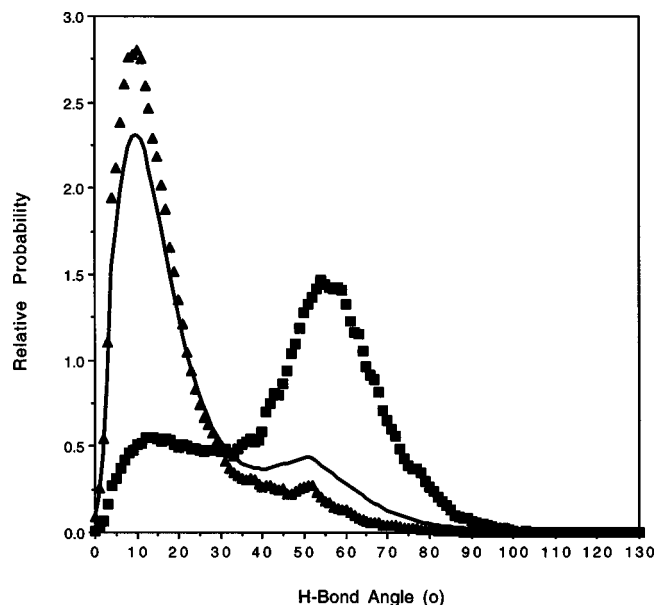


FIG. 3. Water–water H-bond angle distribution at 25 °C for pure water (—), for the first hydration shell of TMAO methyl groups (\blacktriangle), and for the first hydration shell of K^+ and Cl^- ions (\blacksquare).

primarily due to water–water H bonds in the first hydration shell of the three methyl groups. For these H bonds there is a shift in population from the high angle peak to the low angle peak (Fig. 3). For both ionic and TMAO solutions the positions of the low and high angle peaks change little compared to pure water. The effect of the solute is primarily on the relative populations. In contrast, urea has no detectable effect on the rms water–water H-bond angle in its first hydration shell, in spite of the presence of the “polar” C=O and NH_2 groups (Table I), and no effect on the relative populations of the low and high angle peaks.

Increases or decreases in the rms H-bond angle between first shell waters are accompanied by increases or decreases, respectively, in the mean H-bond length (Table I). These changes are highly correlated ($R^2=0.994$) but the changes in length are much smaller than the changes in angle. For the solutes studied here the H-bond length varied by only 8% while the rms angle varied by more than a factor of 2.

IV. DISCUSSION

Our major observations from the simulations and IR spectroscopy can be summarized as follows. The primary structural effect of the addition of the ionic solutes to water is to increase the rms water–water H-bond angle in the first hydration shell. There is a concomitant shift to higher frequency in the OH stretching mode, and a downward shift in the HOH bending mode frequency. In contrast, the hydrophobic solute TMAO decreases the rms water–water H-bond angle in its first hydration shell, shifts the OH stretching mode frequency lower, and shifts the HOH bending mode frequency up. Urea has no effect on the rms H-bond angle, OH stretch, and HOH bend frequencies. Given the observation from simulations that in pure water there is a bimodal distribution of H-bond angles, both structural and spectroscopic results can be satisfactorily explained in terms of

changes in the relative proportions of these two H-bond angle populations. The addition of the ionic solutes increases the population of more distorted H bonds relative to the less distorted population, TMAO has the reverse effect, while urea does not affect the H-bond population distribution.

Deconvolution and assignment of IR spectra are not straightforward. Nevertheless, the fact that all the spectra can be fit by two peaks at fixed frequencies (3350 and 3450 cm^{-1}) but varying intensities is consistent with the simulation results: That there are “two populations” of H-bond angles, and the effect of solutes is to change the relative amounts. Moreover, the direction of the effect is consistent with the simulations. The hydrophobic solute increases the population of less distorted H bonds, lowers the rms H-bond angle and length, and increases the relative intensity of the lower-frequency component of the spectrum. Conversely, ionic solutes increase the population of the more distorted H bonds, increasing the rms H-bond angle and length, thereby expanding the relative intensity of higher-frequency component of the spectrum. The direction of all these effects is what one expects on physical grounds. In addition, the relative size of the effects of the ionic solutes on the spectra is explained by the simulation results: At constant molality, the effect on the spectrum is larger for KSCN than for KCl and NaCl, while the effects of the latter two salts are very similar. An examination of Table I shows that this is because SCN^- is a larger ion than Cl^- , so there are more H bonds perturbed in the first shell, even though the degree of perturbation is not as large as for Cl^- . KCl and NaCl have similar effects since the number of H bonds, and the degrees of distortion are similar. Bending mode frequency shifts induced by the different solutes are in all cases opposite to the stretching frequency shifts (Table I). Again, this is consistent with the simulated shift in populations of less distorted and more distorted H bonds.

Support for the idea that there are different classes of H bonds in water comes also from previous spectroscopic studies. Laenen *et al.*^{15,16} argue that the OH stretch is composed of a more “icelike” contribution at lower frequency, with a longer reorientation time, and higher-frequency contributions involving “weaker” H bonding with smaller reorientation times. However, they further decomposed the latter contribution into two spectral components. Ratcliffe *et al.*¹⁷ studied the temperature dependence of the Raman spectrum of liquid water, and concluded that their observations are consistent with a model in which the vibrational bands consisted of components representing strong and weak H bonds. They also pointed out that their results were not compatible with a two-state water mixture-type model in which icelike clusters exist in a “sea of relatively free nonhydrogen bonded water.” Our simulations also do not show two classes of water, but a single population of water that partakes in “two” classes of H bonds.

James *et al.*¹⁸ studied librational bands (low-frequency) of water solutions with electrolytes and nonelectrolytes (urea, formamide, tetraalkylammonium nitrates). In particular, they point out that urea both downshifts the band (meaning the degree of H bonding is decreasing), and simultaneously increases the intensity of the highest-frequency

component (the most strongly H bonded. The authors attribute the latter to “complete” tetrahedral H bonding. They conclude that urea is both structure “making” and “breaking.” This conclusion is supported by our previous simulations of urea, where its small net effect on water structure results from opposing effects of the NH₂, C, and O groups.⁶

In spite of this consistency with experiment, one must be cautious in identifying the two peaks in the deconvoluted spectra too literally with the two populations of H-bond angles seen in the simulations: First, the deconvolution of the spectra is not unique because there are no clearly resolved peaks. Even if there were, this would not imply that each component in the deconvolution corresponds to a “single IR species.” Finally, it is not at this time possible to relate a particular IR peak to a given water-pair/H-bond configuration or configurations due to the difficulty of *ab initio* IR spectrum calculations.

These difficulties do not change the central conclusions to be drawn from this work: A combination of IR spectroscopy and simulations is a useful way to study the effect of solutes on water structure. The addition of hydrophobic groups to water decreases the angular distortion of water–water H bonds, while the addition of polar and ionic groups increases the angular distortion. These changes in the angular distortion of H bonds are the primary effect of small solutes on water structure.

Finally, after much discussion in the literature of the mechanism of the denaturing properties of urea, the IR spectroscopy and our simulations show that urea does not significantly alter the H-bond structure of water, as judged by the distribution of water–water H-bond angles, a sensitive structural probe of water. This is consistent with results from earlier simulations,^{19,20} where an analysis of radial distribution functions of water and solute–water also revealed little change in water structure. In our simulations the net neutral effect on the water structure of urea results from a cancellation of increases and decreases in H-bond angle caused by the different moieties NH₂, C, and O.⁶ This ambivalent effect of urea is consistent with its measured ability to bind favorably to both peptide backbone and hydrophobic sidechain groups.^{21,22} These experimental studies, the work described here, and previous simulations^{23,24} provide strong support for the direct binding model for protein denaturation.

We can ask further why binding of urea is so effective at unfolding a protein. Taking as an implication of the IR spectroscopy and simulations that the strength of individual

urea–water and water–water H bonds (and thus peptide–water H bonds) are essentially the same, the H bonding between peptide groups and between water molecules is basically in competition. However, urea can H bond to both the peptide C=O and NH. Since the energy difference between *cis* and *trans* peptides is only about 2.5 kcal/mole,²⁵ this bidentate H-bonding interaction would greatly increase the propensity for the peptide bond to be in the *cis* position. Since in the secondary structure elements of the native protein, the group is in the *trans* position, the H-bonding pattern favored by urea destabilizes the protein structure.

ACKNOWLEDGMENTS

We gratefully acknowledge support from the National Institute of Health Grants No. R01-GM54105 (K.A.S. and B.M.), No. R01-GM55004, and No. PO1-GM48130 (J.V., E.M.).

- ¹D. Eisenberg and W. Kauzmann, *The Structure and Properties of Water* (Oxford University Press, Oxford, 1969).
- ²B. Madan and K. A. Sharp, *J. Phys. Chem.* **100**, 7713 (1996).
- ³B. Madan and K. A. Sharp, *J. Phys. Chem.* **101**, 11237 (1997).
- ⁴B. Madan and K. Sharp, *Biophys. Chem.* **78**, 33 (1999).
- ⁵K. A. Sharp and B. Madan, *J. Phys. Chem.* **101**, 4343 (1997).
- ⁶F. Vanzi, B. Madan, and K. Sharp, *J. Am. Chem. Soc.* **120**, 10748 (1998).
- ⁷J. Turner, *Mol. Phys.* **70**, 679 (1990).
- ⁸J. Turner and A. Soper, *J. Chem. Phys.* **101**, 6116 (1994).
- ⁹J. Turner, A. Soper, and J. Finney, *J. Chem. Phys.* **102**, 5438 (1995).
- ¹⁰B. Madan and K. A. Sharp (unpublished).
- ¹¹A. Wang and D. W. Bolen, *Biochemistry* **36**, 9101 (1997).
- ¹²J. Wright, M. Laberge, and J. Vanderkooi, *Biochemistry* **36**, 14724 (1997).
- ¹³W. L. Jorgensen and J. Tirado-Rives, *J. Am. Chem. Soc.* **110**, 1657 (1988).
- ¹⁴W. L. Jorgensen, BOSS, Version 3.3, Copyright Yale University, New Haven, CT, 1992.
- ¹⁵R. Laenen, C. Rauscher, and A. Laubereau, *J. Phys. Chem. B* **103**, 9304 (1998).
- ¹⁶R. Laenen, C. Rauscher, and A. Laubereau, *Phys. Rev. Lett.* **80**, 2622 (1998).
- ¹⁷C. I. Ratcliffe and D. E. Irish, *J. Phys. Chem.* **86**, 4897 (1982).
- ¹⁸D. W. James, R. F. Armishaw, and R. L. Frost, *J. Phys. Chem.* **80**, 1346 (1976).
- ¹⁹R. Kuharski and P. Rossky, *J. Am. Chem. Soc.* **106**, 5786 (1984).
- ²⁰A. Wallqvist, D. Covell, and D. Thirumalai, *J. Am. Chem. Soc.* **120**, 427 (1998).
- ²¹A. J. Wang and D. W. Bolen, *Biophys. J.* **70**, SuAM7 (1996).
- ²²Q. Zou, S. Habermann, and K. P. Murphy, *Proteins* **31**, 107 (1997).
- ²³J. W. Wu and Z. X. Wang, *Protein Sci.* **8**, 2090 (1999).
- ²⁴A. Cafisch and M. Karplus, *Struct. Folding Des.* **7**, 477 (1999).
- ²⁵T. Drakenberg and S. Forsen, *Chem. Soc. Chem. Commun.* **71**, 1404 (1971).